Polymer Journal (2024) 56:319–333
https://doi.org/10.1038/s41428-023-00848-8

ORIGINAL ARTICLE

Investigation of the mechanical properties and degradation of ester-free poly(trimethylene carbonate) derivatives bearing various bulky aromatic groups

Rikyu Miyake[1] · Hiroharu Ajiro[1,2]

Received: 3 September 2023 / Revised: 8 October 2023 / Accepted: 22 October 2023 / Published online: 1 December 2023

Abstract

Ester-free trimethylene carbonate derivatives bearing bulky aromatic groups were designed and synthesized, including those with one or two benzyl groups, diphenylmethyl groups, and triphenylmethyl groups. The polymerization reactions of these monomers were investigated with several initiators. The mechanical properties of the polymers were determined with compressive tests, resulting in approximately 0.3 MPa at most. The degradation behaviors were also evaluated in lipase solutions and aqueous 0.01 M NaOH for several weeks, which revealed that the substituents impeded degradation in most cases. The degradation processes were slow, and they were analyzed with weight loss, SEM, SEC, TGA, and DSC studies.

Introduction

Most polymeric materials are chemically stable, so it is extremely difficult for them to degrade into low molecular weight compounds in natural environments, such as soils and the ocean. As a result, plastic waste has been accumulating worldwide in recent years, leading to concerns about environmental pollution [1]. Furthermore, environmental pollution caused by microplastics originating from synthetic polymer materials is also a growing concern [2]. Microplastics are plastic particles with sizes less than 5 mm [3], and they are generated through radical reactions induced by heat, light, and water in the natural environment [4, 5]. Microplastics are light and durable, so they are easily carried by currents, and their accumulation in oceans and rivers causes environmental pollution [6–8]. Microplastics adsorb harmful heavy metals, organic pollutants, and bacteria on their surfaces, which is why marine pollution is a significant concern [4, 9]. When microplastics with attached harmful substances enter the bodies of marine plankton, abnormal effects occur, leading to a decrease in the population of marine plankton and potential ecosystem disruption [10, 11]. Additionally, marine organisms that ingest microplastics may undergo biomagnification, in which harmful substances concentrated on the microplastic surfaces accumulate within their bodies [12]. This raises concerns about adverse effects on human health if humans consume fish and other organisms that have accumulated harmful substances from microplastics [13].

Considering this background, research on biodegradable polymers has gained significant momentum in recent years as part of effort to achieve the Sustainable Development Goals (SDGs) [14, 15]. Biodegradable polymers are polymers that, when exposed to the natural environment and microbial activity, break down into natural byproducts such as water and carbon dioxide [14]. There are two main categories of biodegradable polymers: those derived from renewable resources, which are called biobased polymers, and those produced from fossil resources, which are petroleum-based polymers. Biobased polymers include materials such as poly(lactic acid) (PLA), which is synthesized from starch sources such as corn and is known for its stiffness and brittleness [16]. Additionally, polymers such as poly(hydroxyalkanoate) (PHA) are synthesized by microorganisms the use plant oils and sugars as the raw materials [17]. On the other hand, petroleum-based

Supplementary information The online version contains supplementary material available at https://doi.org/10.1038/s41428-023-00848-8.

✉ Hiroharu Ajiro
ajiro@ms.naist.jp

[1] Division of Materials Science, Nara Institute of Science and Technology, 8916-5 Takayama-cho, Ikoma, Nara 630-0192, Japan

[2] Data Science Center, Nara Institute of Science and Technology, 8916-5 Takayama-cho, Ikoma, Nara 630-0192, Japan

polymers include a range of materials, including poly(-butylene succinate) (PBS) with high heat resistance [18], poly(glycolic acid) (PGA) with excellent gas barrier properties [19, 20], polycaprolactone (PCL) with exceptional flexibility and elasticity [21], and polybutylene adipate terephthalate (PBAT), which is known for its flexibility, strength, and resistance to hydrolysis [22]. These biodegradable polymers have various applications, such as the PLA in foam sheets [23] and the PBS in agricultural films [24, 25]. Due to their biodegradabilities, they are considered environmentally friendly and potential contributors in addressing the issues of microplastics. However, these biodegradable polymers contain ester bonds in their polymer backbone, which can lead to the generation of acidic organic compounds, particularly carboxylic acids, during degradation processes [26, 27]. These acidic organic compounds might pose a risk of environmental acidification, including soils and oceans, under certain circumstances.

On the other hand, poly(trimethylene carbonate) (PTMC) is a biodegradable polymer that contains carbonates in its backbone instead of esters. PTMC is obtained via ring-opening polymerization of trimethylene carbonate (TMC). It exhibits biodegradability, biocompatibility, and flexibility [28–30], and its side chains are easily modified [31]. Furthermore, it ultimately generates environmentally friendly compounds, namely, carbon dioxide and 1,3-propanediol, through hydrolysis during degradation [32, 33]. Unlike PLA or PCL, PTMC maintains a neutral pH during degradation, so it has minimal environmental impact and is suitable for natural environments such as soils and the ocean and as a medical material less prone to the inflammation caused by acidic organic compounds [34, 35]. Recent research has delved into the degradation processes of PTMC derivatives in some detail [36–38]. However, PTMC is an amorphous polymer with a low mechanical strength [29], so ingenuity is required for application as a material. To introduce functionality in the monomer, studies have been actively conducted on PTMC derivatives with substituents attached with ester bonds to the side chains [39–41]. Nevertheless, PTMC derivatives with ester bonds in their side chains generate acidic organic compounds during degradation [42], which limits the use of PTMC and its neutrality during degradation, as we have perceived.

We previously synthesized ester-free PTMC derivatives by introducing substituents into the side chains without using ester bonds. This was inspired by the oral rat LD50 values of the commercially available 2,2-bis(hydroxymethyl)propionic acid and trimethylolethane, which are the starting materials for both ester-type and ester-free PTMC derivatives. These starting materials are produced by hydrolysis. For instance, PTMC derivatives with oligo(ethylene glycol) (OEG) side chains have exhibited unique degradation behaviors distinct from that of PTMC, including sharp thermoresponsive behavior near body temperature [43]. In enzymatic solutions, they exhibit slow degradation, while in basic aqueous solutions, they degrade differently [44]. Additionally, PTMC derivatives with OEG side chains are low-viscosity liquids, so their individual use is challenging. However, we have synthesized transparent and highly flexible hydrogels with crosslinking agents [45]. Furthermore, in the syntheses of monomers with aromatic substituents in the side chains, we established a three-step monomer synthetic pathway [46]. We have also discovered that monomers with trityl groups in the side chains can be synthesized in just two steps [47]. Introduction of aromatic substituents into the side chains has led to improvements in polymer characteristics such as the glass transition temperature and thermal decomposition temperature [48]. Various PTMC derivatives with different functionalities have been developed as described above. However, knowledge of the polymer properties, such as the mechanical and degradation characteristics, remains insufficient. Additionally, in our previous reports, many polymers had number-average molecular weights below 10,000, which poses challenges because their polymer chains may not intertwine adequately.

In this study, our aim was to synthesize ester-free PTMC derivatives with bulky substituents, such as aromatic substituents, and investigate their properties. We have set out to determine how the chemical structures of the side chains influenced the polymer properties. Furthermore, we aimed to reveal how differences in the side chain substituents affect the properties of the PTMC derivatives and explore their degradation processes.

Experiments

Materials

Trimethylolethane, *p*-toluenesulfonic acid monohydrate, ethyl chloroformate, triethylamine, trityl bromide, 1,3-dioxan-2-one, benzyl bromide, (bromomethylene)dibenzene, pentaerythritol, tin(II) 2-ethylhexanoate, dibutyltin oxide and potassium *tert*-butoxide (12% in THF, ca. 1 mol/L) were purchased from Tokyo Chemical Industry Co. Ltd. (Tokyo, Japan) *N,N*-dimethyl-4-aminopyridine was purchased from Wako Pure Chemical Industries, Ltd. (Osaka, Japan). Dulbecco's phosphate buffered saline (PBS) (-) solution without Ca and Mg (10×) was purchased from Nacalai Tesque. Ltd., and used after dilution with ultrapure water. Lipase from Candida rugosa Type VII, ≥700 unit/mg solid, was purchased from Sigma-Aldrich Japan Co. Ltd. (Tokyo, Japan). Anhydrous dichloromethane, anhydrous *N,N*-dimethylformamide (DMF), and anhydrous tetrahydrofuran (THF) were purchased from Kanto Chemical Co. Inc. (Tokyo, Japan).

Synthesis of 2-{(Benzyloxy)methyl}-2-methylpropane-1,3-diol (Diol-pend-Ph)

Diol-pend-Ph was synthesized as follows, and it was analyzed as described in the literature[49]. Trimethylolethane (0.756 g, 6.00 mmol) and KOH (1.12 g, 20.0 mmol) were added to a 100 mL two-neck flask, followed by the addition of 5.0 mL of DMF under a nitrogen atmosphere. While keeping the reaction mixture on ice, benzyl bromide (2.39 ml, 20.0 mmol) was added, and the mixture was stirred overnight at 60 °C. Subsequently, an extraction was performed with a saturated NaCl aqueous solution and a mixed solvent of hexane/EtOAc = 3/1 (v/v), and the organic layer was collected. Magnesium sulfate ($MgSO_4$) was added to the collected organic layer and filtered, and the solvent was removed. Purification was achieved through silica gel column chromatography with EtOAc/hexane (1/3, v/v), yielding a white solid compound, **Diol-pend-Ph** (2.52 g, 12.0 mmol, 59.9%).

Synthesis of 5-{(Benzyloxy)methyl}-5-methyl-1,3-dioxan-2-one (TMCM-Ph)

TMCM-Ph was synthesized in accordance with the literature[46]. **Diol-pend-Ph** (3.45 g, 16.4 mmol) was dissolved in 40 mL of THF, and the resulting solution was dried over MS4A. This mixture was then added to a 200 mL two-neck flask under a nitrogen atmosphere. Ethyl chloroformate (4.69 mL, 49.2 mmol) was added, and the reaction was cooled to 0 °C in an ice bath. Triethylamine (6.86 mL, 49.2 mmol) was then added dropwise, and the mixture was stirred for 5 hours. Extraction was carried out with ion-exchanged water and CH_2Cl_2, and the organic layer was collected. $MgSO_4$ was added to remove water, the collected organic layer was filtered, and the solvent was removed. Recrystallization was performed in EtOAc and hexane, resulting in the white solid **TMCM-Ph** (2.33 g, 9.85 mmol, 60.0%).

Synthesis of 2-{(Benzhydryloxy)methyl}-2-methylpropane-1,3-diol (Diol-pend-Bp)

Diol-pend-Bp was synthesized in accordance with the literature[46]. Trimethylolethane (2.17 g, 18.0 mmol), (bromomethylene)dibenzene (1.48 g, 6.00 mmol), and *N,N*-dimethyl-4-aminopyridine (0.0733 mg, 0.600 mmol) were added to a 200 mL three-neck flask, and the system was purged with nitrogen. Subsequently, 4.5 mL of DMF and 0.836 mL of triethylamine (6.00 mmol) were added, and the mixture was stirred overnight at 60 °C. Afterward, extraction was carried out with ion-exchanged water and a mixed solvent of hexane/EtOAc (3/1, v/v), and the organic layer was collected. $MgSO_4$ was added to the collected organic layer and filtered, and the solvent was removed. Purification was achieved through silica gel column chromatography with EtOA/hexane (1/1, v/v), yielding a white solid compound, **Diol-pend-Bp** (1.33 g, 4.65 mmol, 77.6%).

Synthesis of 5-{(Benzhydryloxy)methyl}-5-methyl-1,3-dioxan-2-one (TMCM-Bp)

TMCM-Bp was synthesized in accordance with the literature[46]. The compound Diol-pend-Bp (0.85 g, 2.99 mmol) was dissolved in 10 mL of THF, and the resulting solution was dried over MS4A. This mixture was then added to a 50 mL two-neck flask under a nitrogen atmosphere. Ethyl chloroformate (0.855 mL, 8.98 mmol) was added, and the reaction was cooled to 0 °C with an ice bath. Triethylamine (1.25 mL, 8.98 mmol) was then added dropwise, and the mixture was stirred for 6 h. Afterward, liquid–liquid extraction was carried out with ion-exchanged water and CH_2Cl_2, and the organic layer was collected. $MgSO_4$ was added to the collected organic layer and filtered, and the solvent was removed. The material was recrystallized from approximately 5 mL of EtOAc and 100 mL of hexane, yielding a white solid compound, TMCM-Bp (0.730 g, 2.34 mmol, 78.2%).

Synthesis of TMCM-TMC

2-{Triphenylmethoxymethyl}-2-methylpropane-1,3-diol (**Diol-pend-Tr**) and 5-{(triphenylmethyloxy)methyl}-5-methyl-1,3-dioxan-2-one (**TMCM-TMC**) were synthesized and analyzed in accordance with the literature[47].

Synthesis of 2,2-Bis((benzyloxy)methyl)propane-1,3-diol (Tetraol-pend-DPh)

Tetraol-pend-DPh was synthesized as follows and was analyzed in accordance with the literature[50]. Pentaerythritol (24.5 g, 180 mmol) and *N,N*-dimethyl-4-aminopyridine (2.20 mg, 18.0 mmol) were added to a 500 mL three-neck flask, and nitrogen purging was performed. Subsequently, 45 mL of DMF, benzyl bromide (43.0 mL, 360 mmol), and triethylamine (24.7 mL, 180 mmol) were added, and the mixture was stirred overnight at 75 °C. Afterward, extraction was carried out with ion-exchanged water and a mixed solvent of hexane/EtOAc (3/1, v/v), and the organic layer was collected. $MgSO_4$ was added to the collected organic layer and filtered, and the solvent was removed. Purification was achieved through silica gel column chromatography with EtOAc/hexane (1/1, v/v), resulting in a white solid compound, **Tetraol-pend-DPh** (6.80 g, 21.5 mmol, 11.9%).

Synthesis of 5,5-Bis((benzyloxy)methyl)-1,3-dioxan-2-one (TMC-DPh)

TMC-DPh was synthesized in accordance with the literature[46]. The compound tetraol-pend-DPh (6.17 g, 19.5 mmol) was dissolved in 45 mL of THF, and the resulting solution was dried over MS4A. This mixture was then added to a 200 mL two-neck flask under a nitrogen atmosphere. Ethyl chloroformate (5.58 mL, 58.6 mmol) was added, and the reaction was cooled to 0 °C with an ice bath. Triethylamine (8.17 mL, 58.6 mmol) was then added dropwise, and the mixture was stirred at room temperature for 5 h. Afterward, extraction was carried out with ion-exchanged water and CH_2Cl_2, and the organic layer was collected. $MgSO_4$ was added to the collected organic layer and filtered, and the solvent was removed. Purification was achieved through silica gel column chromatography with EtOAc/hexane (1/3, v/v), and recrystallization was performed from approximately 10 mL of EtOAc and 100 mL of hexane to obtain a white solid compound, **TMC-DPh** (5.01 g, 14.7 mmol, 75.1%).

Synthesis of 2,2-Bis((benzhydryloxy)methyl) propane-1,3-diol(Tetraol-pend-DBp)

Pentaerythritol (4.08 g, 30.0 mmol), (bromomethylene) dibenzene (14.8 g, 60.0 mmol), and *N,N*-dimethyl-4-aminopyridine (0.367 mg, 3.00 mmol) were added to a 200 mL three-neck flask, and nitrogen purging was performed. Subsequently, 30 mL of DMF and triethylamine (4.12 mL, 30.0 mmol) were added, and the mixture was stirred overnight at 75 °C. Afterward, a liquid–liquid extraction was carried out with ion-exchanged water and a mixed solvent of hexane/EtOAc (3/1, v/v), and the organic layer was collected. $MgSO_4$ was added to the collected organic layer and filtered, and the solvent was removed. Purification was achieved through silica gel column chromatography with EtOAc/hexane (1/1, v/v), resulting in a white solid compound, **Tetraol-pend-DBp** (2.78 g, 5.93 mmol, 19.8%). ^{1}H NMR (400 MHz, $CDCl_3$): δ (ppm) = 2.44 (t, 2H, J = 6.2 Hz), 3.57 (s, 4H), 3.75 (d, 4H, J = 6.0 Hz), 5.31 (s, 2H), 7.23–7.32 (m, 20H). FT-IR (cm^{-1}): 3285, 2864, 1493, 1452, 1308, 1273, 1180, 1153, 1101, 1057, 1024, 1005, 920, 868, 835, 767, 741, 706, 693. MS (MALDI): calcd. For $C_{31}H_{32}O_4$ $[M+Na]^+$ 491.22; found 491.22.

Synthesis of 5,5-bis((benzhydryloxy)methyl)-1,3-dioxan-2-one(TMC-DBp)

The compound **Tetraol-pend-DBp** (2.08 g, 4.44 mmol) was dissolved in 10 mL of THF, and the resulting solution was dried over MS4A. This mixture was then added to a 200 mL two-neck flask under a nitrogen atmosphere. Ethyl chloroformate (1.27 mL, 13.3 mmol) was added, and the reaction was cooled to 0 °C with an ice bath. Triethylamine (1.83 mL, 13.3 mmol) was then added dropwise, and the mixture was stirred at room temperature for 5 h. Afterward, extraction was carried out with ion-exchanged water and CH_2Cl_2, and the organic layer was collected. $MgSO_4$ was added to the collected organic layer and filtered, and the solvent was removed. Purification was achieved through silica gel column chromatography with EtOAc/hexane (1/3, v/v), and recrystallization was performed from approximately 10 mL of EtOAc and 100 mL of hexane cooled to −30 °C. The mixture was then filtered, resulting in a white solid compound, **TMC-DBp** (1.56 g, 3.17 mmol, 71.5%). ^{1}H NMR (400 Hz, $CDCl_3$): δ (ppm) = 3.54 (s, 4H), 4.38 (s, 4H), 5.31 (s, 2H), 7.23–7.33 (m, 20H). FT-IR (cm^{-1}): 3024, 2918, 1755, 1599, 1493, 1454, 1406, 1348, 1323, 1278, 1247, 1176, 1109, 1076, 1020, 993, 868, 739, 695. MS(MALDI) calcd. For $C_{32}H_{30}O_5$ $[M+Na]^+$: 494.20; found 494.59.

Synthesis of 2,2-Bis((trityloxy)methyl)propane-1,3-diol (Tetraol-pend-DTr)

Pentaerythritol (4.08 g, 30.0 mmol), trityl bromide (19.4 g, 60.0 mmol), and *N,N*-dimethyl-4-aminopyridine (0.733 mg, 6.00 mmol) were added to a 200 mL three-neck flask, and nitrogen purging was performed. Subsequently, 50 mL of DMF and triethylamine (8.36 mL, 60.0 mmol) were added, and the mixture was stirred overnight at 75 °C. Afterward, extraction was carried out using ion-exchanged water and a mixed solvent of hexane/EtOAc (3/1, v/v), and the organic layer was collected. $MgSO_4$ was added to the collected organic layer and filtered, and the solvent was removed. Purification was achieved through silica gel column chromatography using EtOAc/hexane (1/1, v/v), resulting in a white solid compound, **Tetraol-pend-DTr** (5.22 g, 8.41 mmol, 28.0%). ^{1}H NMR (400 MHz, CDCl3): δ (ppm) = 2.01 (t, 2H, J = 6.4 Hz), 3.34 (s, 4H), 3.61 (d, 4H, J = 6.40 Hz), 7.15–7.39 (m, 30H). FT-IR (cm^{-1}): 3406, 3057, 2926, 2882, 2363, 1489, 1447, 1317, 1219, 1182, 1153, 1068, 1032, 984, 899, 764, 745, 696, 633. MS(MALDI) calcd for $C_{43}H_{40}O_4$ $[M+Na]^+$: 643.79; found 643.28.

Synthesis of 5,5-bis((trityloxy)methyl)-1,3-dioxan-2-one (TMC-DTr)

The compound **Diol-pend-Tr** (5.22 g, 8.41 mmol) was dissolved in 45 mL of THF, and the resulting solution was dried over MS4A. This mixture was then added to a 200 mL three-neck flask under a nitrogen atmosphere. Ethyl chloroformate (2.40 mL, 25.2 mmol) was added, and the reaction was cooled to 0 °C using an ice bath. Triethylamine

(3.52 mL, 25.2 mmol) was then added dropwise, and the mixture was stirred for 5 h. After removing the solvent from the reaction mixture, liquid–liquid extraction was performed using ion-exchanged water and CH_2Cl_2, and the organic layer was collected. $MgSO_4$ was added to the collected organic layer and filtered, and the solvent was removed. Recrystallization was carried out using 50 mL of EtOAc and 1000 mL of hexane, followed by centrifugation (3 min, 3500 rpm, 25 °C), resulting in a white solid compound, **TMC-DTr** (4.62 g, 7.15 mmol, 85.0%). ^{1}H NMR (400 Hz, $CDCl_3$): δ (ppm) = 3.32 (s, 4H), 4.21 (s, 4H), 7.12–7.32 (m, 30H). FT-IR (cm^{-1}): 3061, 3022, 1763, 1595, 1489, 1447, 1396, 1248, 1223, 1171, 1117, 1074, 1032, 997, 979, 897, 853, 766, 746, 696, 633. HRMS calcd. For $C_{20}H_{23}O_5$ $[M+Na]^+$: 669.77; found 669.26.

Polymerization with $SnOct_2$ as the initiator

All monomers were recrystallized from EtOAc/hexane before polymerization. The polymerizations were conducted at temperatures above their melting points with $SnOct_2$ used as the catalyst. The polymerizations were carried out at 160 °C, except for that of **TMC-DTr**, which was carried out at 220 °C because its melting point is 217 °C and the boiling point of $SnOct_2$ is 228 °C. A 30 mL Schlenk tube was heated with a heat gun and dehydrated under vacuum before use. The monomers (0.500 g) were added to a 30 mL Schlenk tube, and $SnOct_2$ was added to achieve a molar ratio of 500:1 between the monomers and the catalyst, followed by nitrogen purging. The mixture was then stirred for 5 h at 160 °C, while TMC-DTr was stirred at 220 °C. After cooling to room temperature, a small amount of CH_2Cl_2 was added to the mixture, followed by precipitation using hexane/2-propanol (9/1, v/v). The precipitate was collected through centrifugation (3500 rpm, 25 °C, 5 min), and the polymer was obtained by removing the solvent.

Polymerization with Bu_2SnO as an initiator

All monomers were recrystallized from EtOAc/hexane before polymerization. The melt polymerizations were conducted at temperatures 40 °C higher than the melting points of the monomers. However, because the decomposition temperature of Bu_2SnO at 162 °C, the synthesis of **TMCM-Tr** was carried out at 150 °C, and no polymerization was performed with **TMC-DTr**, considering their melting points. First, the monomers were vacuum-dried at room temperature overnight. Additionally, a 30 mL Schlenk tube was heated and dehydrated using a heat gun under vacuum before use. The monomers (0.500 g) were added to a 30 mL Schlenk tube, and Bu_2SnO was added to achieve a molar ratio of 250:1 between the monomers and the catalyst, followed by nitrogen purging. The mixture was then stirred for 5 h at the specified temperature. After cooling to room temperature, a small amount of CH_2Cl_2 was added to the mixture, followed by precipitation with methanol. The precipitate was collected through centrifugation (3500 rpm, 25 °C, 5 min), and the polymer was obtained by removing the solvent.

Polymerization with *t*-BuOK as the initiator

All monomers were recrystallized from EtOAc/hexane before polymerization. Before polymerization, the samples were vacuum dried at room temperature overnight. Additionally, a 30 mL Schlenk tube was heated and dehydrated using a heat gun under vacuum before use. The monomers (0.500 g) were added to a 30 mL Schlenk tube, and nitrogen purging was performed. Then, a predetermined amount of THF was added to dissolve the monomers, and the mixture was cooled with ice. A 0.1 M solution of *t*-BuOK in THF was prepared as the initiator solution, and the ratio of monomer to initiator was adjusted to 100:1 by adding the *t*-BuOK solution to a 30 mL Schlenk tube. The mixture was allowed to stand at an ice-cold temperature for a specified time. A small amount of THF was added to the mixture, followed by precipitation with methanol. The precipitate was collected through centrifugation (3500 rpm, 25 °C, 5 min), and the polymer was obtained by removing the solvent.

Characterization

Proton nuclear magnetic resonance (^{1}H NMR) spectra were measured with a JEOL JNM-GSX400 system. The number-average molecular weights (M_n) and polydispersity indexes ($Đ$) of the polymers were estimated with size exclusion chromatography (SEC). The SEC system was composed of an RI-2031 Plus Intelligent RI detector, a PU-2080 Plus Intelligent HPLC pump, an AS-2055 Plus Intelligent Sampler, a CO-2065 Plus Intelligent Column oven (JASCO Co. Ltd.), and a commercial column (TSKgel Super3000 and GMHXL, Tosoh Co. Ltd.). The system was controlled with a polystyrene standard using THF as the eluent at 40 °C. FT-IR/ATR spectra were measured with a Spectrum 100 FT-IR spectrometer (PerkinElmer) and IRAffinity-1S ATR Miracle A (Shimadzu). X-ray diffraction (XRD) patterns were measured with a Rigaku RINT-TTRIII/NM system. Cu Kα ($\lambda = 154$ nm) was used as the X-ray source and operated at 50 kV and 300 mA with a Ni filter at $2\theta = 5°$–$40°$ with a scan speed of 0.5°/min. Thermogravimetric analyses (TGA) were performed with a TGA-50 system (Shimadzu Corporation, Japan) under a nitrogen atmosphere with a heating rate of 10 °C/min. Differential scanning calorimetry (DSC) was performed with a DSC-60 Plus and TAC/L system with heating and cooling rates of

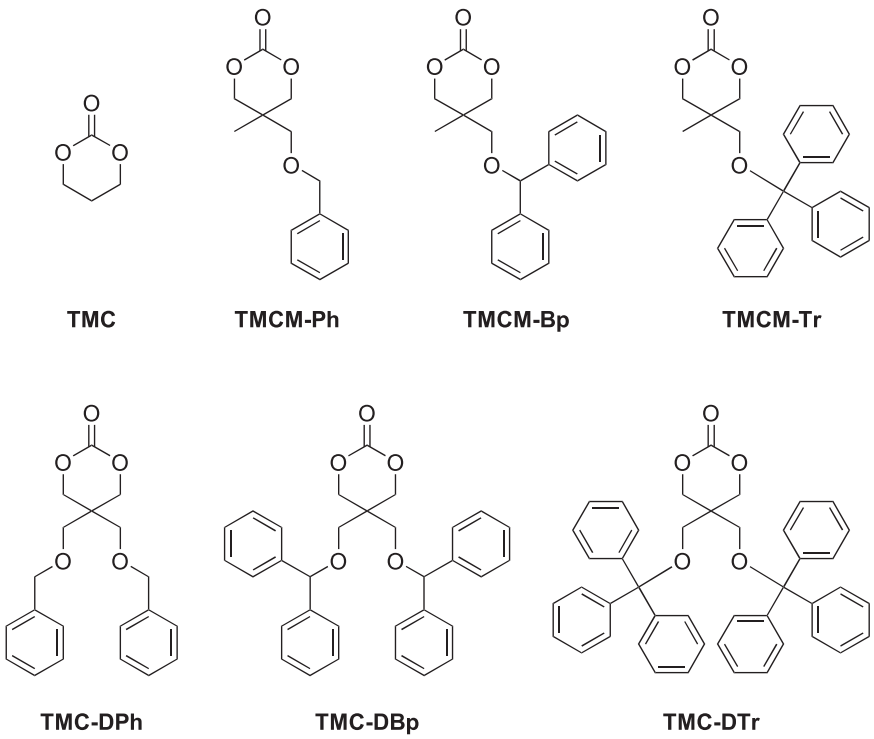

Fig. 1 Chemical structures of the TMC and ester-free TMC derivatives bearing various bulky aromatic groups used in this study

5 °C/min. The DSC data for all samples showed the 1st scan, and the melting points ™ of the samples were obtained. The compressive tests were achieved with the EZ-test system controlled by TRAPEZZIUM LITE X (Shimadzu Corp. Japan).

Results and discussion

The chemical structures of TMC and the ester-free TMC derivatives bearing bulky aromatic groups are shown in Fig. 1. Synthetic routes to these monomers that did not require protecting most of the hydroxyl groups were used in this study (Supplementary Fig. S1) because the bulky groups prevented substitution reactions at all positions, although other synthetic routes have been reported with protecting steps [43, 46]. In all of the TMC derivatives, the disappearance of hydroxyl peaks for the diol derivatives and the shifts of methylene peaks adjacent to hydroxyl peaks from diol derivatives to TMC derivatives in ^{1}H NMR spectra, as well as the disappearance of hydroxyl stretching peaks for the diol derivatives and the appearance of carbonyl stretching peaks for the TMC derivatives in FT-IR spectra, were observed (Supplementary Figs. S2–S11).

Previously, we used DBU as a catalyst [51] for polymerization of the TMC derivatives, but the M_n results showed low weights of a few thousand Daltons. High molecular weights for PTMC have been obtained with tin catalysts [52–54], as well as *t*-BuOK [55] for TMC derivatives bearing bulky groups. Therefore, we tried polymerization with those catalysts. Since polymerization with the tin catalyst required a high temperature that melted the monomer, the thermal degradation temperature (T_d) and the melting points (T_m) of the TMC derivatives were determined with TGA and DSC studies (Table 1). The bulkier groups of the TMC derivatives led to higher thermal stabilities. The polymerization temperatures were set after considering each T_d and T_m value, although they were not the same polymerization temperatures. The polymerizations were performed with $Sn(Oct)_2$ and Bu_2SuO used as the catalysts, and the results are shown in Table 2.

Table 1 Thermal properties of the TMC derivatives

Entry	Monomer	T_d [a] °C	T_m [b] °C
1	**TMCM-Ph**	177	43
2	**TMCM-Bp**	220	115
3	**TMCM-Tr**	204	143
4	**TMC-DPh**	183	79
5	**TMC-DBp**	212	91
6	**TMC-DTr**	294	217

[a]Determined by TGA under nitrogen (10 °C/min)

[b]Determined by DSC during the 1st heating (10 °C/min)

In the case of polymerizations with $SnOct_2$, no hexane/2-propanol insoluble species were obtained from **TMCM-Ph, TMCM-Bp, TMC-DPh**, and **TMC-DTr**, while poly(**TMCM-Tr**) and poly(**TMC-DBp**) exhibited M_n

Table 2 Polymerization of the TMC derivatives with tin catalysts[a]

Entry	Catalyst	Monomer	Temp. °C	Yield[b]%	M_n[c]×10^3	DP[c]	$Đ$[c]
1	$SnOct_2$	**TMCM-Ph**	160	<1	N.D.	N.D.	N.D.
2	$SnOct_2$	**TMCM-Bp**	160	<1	N.D.	N.D.	N.D.
3	$SnOct_2$	**TMCM-Tr**	160	64	4.3	11	1.50
4	$SnOct_2$	**TMC-DPh**	160	<1	N.D.	N.D.	N.D.
5	$SnOct_2$	**TMC-DBp**	160	45	6.7	14	1.33
6	$SnOct_2$	**TMC-DTr**	220	<1	N.D.	N.D.	N.D.
7	Bu_2SnO	**TMCM-Ph**	80	89	15.0	64	1.93
8	Bu_2SnO	**TMCM-Bp**	155	73	21.0	67	1.49
9	Bu_2SnO	**TMCM-Tr**	150	78	3.6	9	1.49
10	Bu_2SnO	**TMC-DPh**	120	45	4.7	14	1.33
11	Bu_2SnO	**TMC-DBp**	130	14	1.9	4	1.10

[a][M]:[I] = 500:1

[b]Hexane/2-propanol (v/v = 9/1) insoluble components (entries 1–6) and MeOH insoluble components (entries 7–11)

[c]Determined by SEC in THF and calibrated with PS standards at 40 °C

Table 3 Polymerization of the TMC derivatives with *t*-BuOK[a]

Entry	Monomer	Conc.mol/L	Time. hr	Yield[b]%	M_n[c] ×10^3	DP[c]	$Đ$[c]
1	**TMCM-Ph**	1.0	0.5	69	23.5	100	1.66
2	**TMCM-Bp**	1.0	0.5	76	21.5	69	1.69
3	**TMCM-Tr**	1.0	0.5	60	10.2	27	1.54
4	**TMCM-Tr**	1.0	1.0	37	6.7	17	1.49
5	**TMCM-Tr**	1.0	2.0	27	7.8	20	1.52
6	**TMCM-Tr**	1.0	4.0	40	7.1	18	1.56
7	**TMC-DPh**	1.0	0.5	64	9.4	30	2.06
8	**TMC-DPh**	1.0	1.0	73	14.3	42	1.64
9	**TMC-DPh**	1.0	2.0	53	13.5	40	1.54
10	**TMC-DBp**	1.0	0.5	26	4.9	10	1.69
11	**TMC-DBp**	1.0	1.0	22	5.6	11	1.46
12	**TMC-DBp**	1.0	2.0	42	6.8	14	1.63
13	**TMC-DBp**	1.0	4.0	36	11.0	22	1.63
14	**TMC-DBp**	1.0	8.0	30	10.9	22	1.75
15	**TMC-DTr**	0.5	0.5	23	2.1	3	1.16
16	**TMC-DTr**	0.5	1.0	10	2.4	4	1.18
17	**TMC-DTr**	0.5	2.0	11	2.5	4	1.23

[a][M]:[I] = 100:1. Initiator = *t*-BuOK. Solvent = THF. Temp. = 0 °C

[b]MeOH insoluble fraction

[c]Determined by SEC in THF and calibrated with PS standards at 40 °C

values of 4300 and 6700, respectively (Table 2, entries 3 and 5). This low reactivity might be due to the prevention of monomer approach to $SnOct_2$ based on the bulkiness of the TMC derivatives and the catalyst active sites for each monomer. The polymerization reactivity was slightly improved by using Bu_2SnO as the catalyst, which provided MeOH insoluble polymers for all TMC derivatives (Table 2, entries 7–11) except for **TMC-DTr** due to the decomposition temperature of Bu_2SnO at T_m for **TMC-DTr**. However, the M_n values were still lower than 10,000 in the cases of poly(**TMCM-Tr**), poly(**TMC-DPh**), and poly(**TMC-DBp**) with relatively bulky side chains (Table 2, entries 9–11).

Next, we used 1.0 M *t*-BuOK in THF as the catalyst, except for 0.5 M with **TMC-DTr** due to its low solubility. The polymerization results are listed in Table 3. The results indicated higher reactivity of the polymerization system with *t*-BuOK and small groups on the growing chains compared to the $SnOct_2$ and Bu_2SnO catalysts. Although MeOH insoluble parts were obtained in any cases, some

polymerizations resulted in low yields, which could be due to an equilibrium between polymerization and depolymerization, or the backbiting reaction. For example, the yield of poly(**TMCM-Tr**) decreased from 60% (Table 3, entry 3) to 27% (Table 3, entry 5) when the polymerization time was increased from 0.5 h to 2.0 h, and the M_n decreased from 10,200 to 7800, indicating that the polymerization was not a living process. Similar behavior was observed for poly(**TMC-DPh**), which showed a decrease in yield from 64% (Table 3, entry 7) to 53% (Table 3, entry 9) and an M_n decrease of 14,300 (Table 3, entry 8) to 13,500 (Table 3, entry 9). The optimal polymerization time seemed to depend on the monomer structure. The yield of poly(**TMC-DBp**) increased from 26% at 0.5 h (Table 3, entry 9) to 42% at 2.0 h (Table 3, entry 12), and M_n increased from 4900 at 0.5 h (Table 3, entry 10) to 11,000 at 4.0 h (Table 3, entry 13), although both the yield and M_n decreased after 8.0 h (Table 3, entry 14). Therefore, the optimized polymerization times for these TMC derivatives were 2 h or less. The poly(**TMC-DTr**) bearing the bulkiest groups exhibited a yield under 23% and M_n under 2500 (Table 3, entries 15–17). It has been reported that bulky substituents led to the formation of cyclic monomers instead of linear polymers [56]. Therefore, optimized polymerization times and concentrations are needed for high yields and high molecular weights.

The polymers with the highest M_n values from each monomer were analyzed with ^{1}H NMR and FT-IR (Supplementary Fig. S12), including poly(**TMCM-Ph**) (Table 3, entry 1), poly(**TMCM-Bp**) (Table 3, entry 2), poly(**TMCM-Tr**) (Table 3, entry 3), poly(**TMC-DPh**) (Table 3, entry 8), poly(**TMC-DBp**) (Table 3, entry 13), and poly(**TMC-DTr**) (Table 3, entry 17). All ^{1}H NMR spectra of the polymers showed singlets for the methylene groups in the polymer backbone at approximately 4.2 ppm, suggesting that the rings of the monomers were opened during polymerization (Fig. 2). The *tert*-butyl groups of the initiator were also observed at the chain ends with signals at approximately 1.45 ppm for all polymers; however, the M_n values calculated from the integrated areas of the peaks for the chain end and main chain did not agree with the theoretical values or the M_n values determined by SEC. For example, the M_n values calculated from ^{1}H NMR spectra of poly(**TMCM-Bp**), poly(**TMCM-Tr**), and

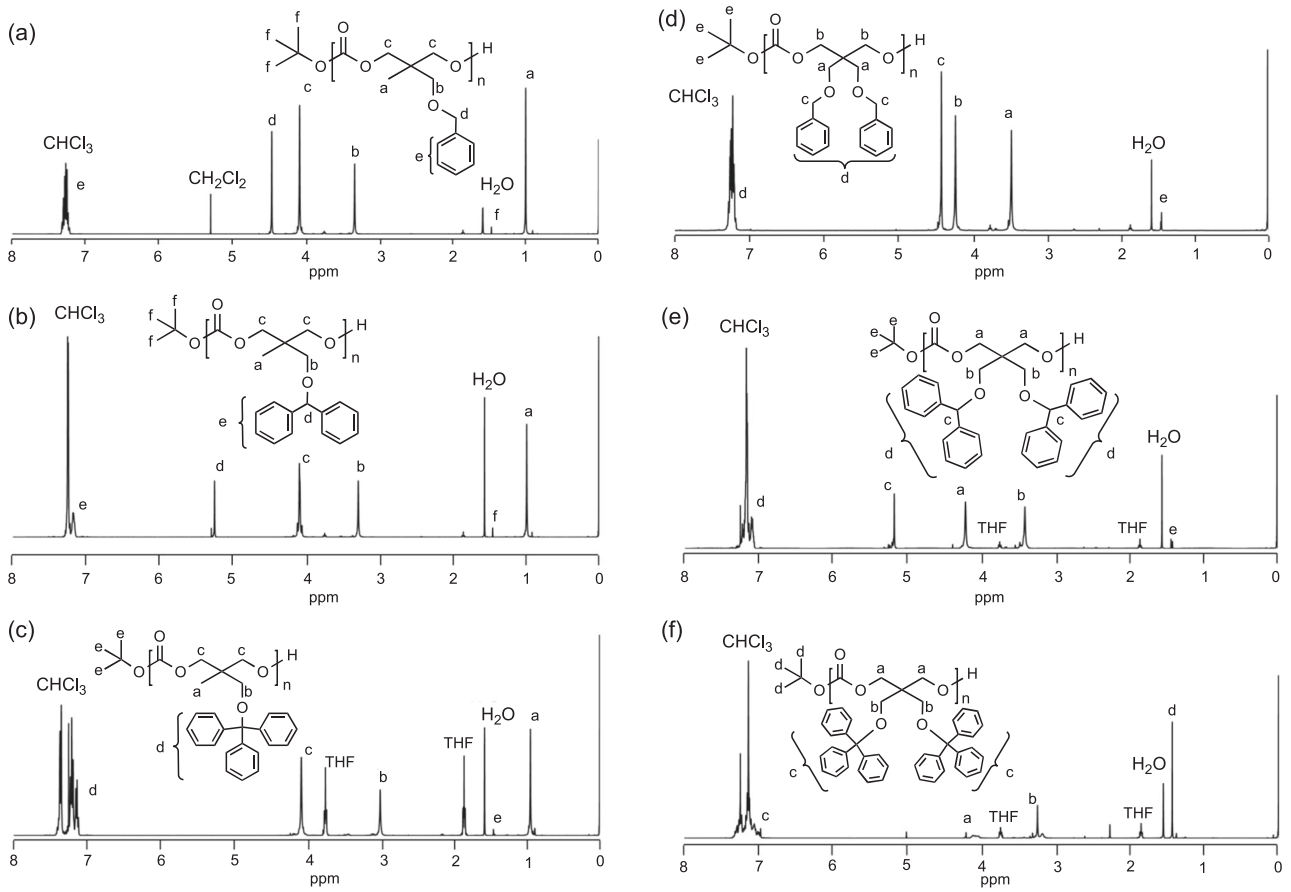

Fig. 2 ^{1}H NMR spectra of ester-free PTMC derivatives bearing bulky aromatic groups and the polymers obtained with *t*-BuOK as the initiator; **a** Poly(**TMCM-Ph**) (Table 3, entry 1). **b** Poly(**TMCM-Bp**) (Table 3, entry 2). **c** Poly(**TMCM-Tr**) (Table 3, entry 3). **d** Poly(**TMC-DPh**) (Table 3, entry 8). **e** Poly(**TMC-DBp**) (Table 3, entry 13) and **f** Poly(**TMC-DTr**) (Table 3, entry 17)

poly(**TMC-DBp**) were 40,600, 43,500, and 24,700, although those determined by SEC were 21,500, 10,200, and 11,000. These results indicate that side reactions, such as intermolecular trans-esterification or back biting [57], residual water initiation and macrocyclic polymer products may have intervened, despite our best procedure for polymerization. This tendency was clearly observed with the bulkier substituents, except for poly(**TMC-DTr**), for which polymerization itself was difficult, although it was also true that the M_n values determined by SEC were relative values based on the PS standards.

Most of the polymers were white solids, whereas poly(**TMCM-Ph**) was a sticky liquid, suggesting that the number of aromatic groups on the side chain contributed to their thermal properties. Some of the 10% weight loss temperatures (T_{10}) for thermal degradation and glass transition temperatures (T_g) have already been reported [46–48], but all polymers prepared with *t*-BuOK in this study were compared. TGA traces of polymers showed T_{10} values between 295 °C and 363 °C, implying that the T_{10} values increased with larger proportions of aromatic moieties (Supplementary Fig. S13). The T_g values for all polymers were determined with DSC, and they were −6 °C, 46 °C, 57 °C, 3 °C, 57 °C, and 73 °C for poly(**TMCM-Ph**), poly(**TMCM-Bp**), poly(**TMCM-Tr**), poly(**TMC-DPh**), poly(**TMC-DBp**), and poly(**TMC-DTr**) (Supplementary Fig. S14). Similarly, increasing numbers of aromatic moieties increased the T_g values, suggesting that they suppressed polymer main mobility.

Next, we evaluated the mechanical properties of the polymers, although those for poly(**TMCM-Ph**) and poly(**TMC-DTr**) could not be measured because poly(**TMCM-Ph**) was liquid and poly(**TMC-DTr**) was too fragile, probably due to the low M_n. Since the rest of the polymers were also somewhat fragile, we decided to evaluate compressive tests instead of tensile tests. Cylinder-shaped samples were prepared by heating with a hot press (Fig. 3). Each polymer was molded at the optimized temperature based on its T_g, T_{10}, and T_m values, because the pellets could not be obtained at low temperatures, and voids were observed at high temperatures. The samples were obtained at temperatures higher than their T_g values: 75 °C for poly(**TMCM-Bp**), 95 °C for poly(**TMCM-Tr**), and 115 °C poly(**TMC-DPh**), and 80 °C for poly(**TMC-DBp**). The compressive test results were compared by using the averages of 7 samples (Fig. 4). A clear fracture stress was not observed for poly(**TMC-DPh**), but the other samples showed fracture stresses within the range 0.06 ± 0.04 MPa

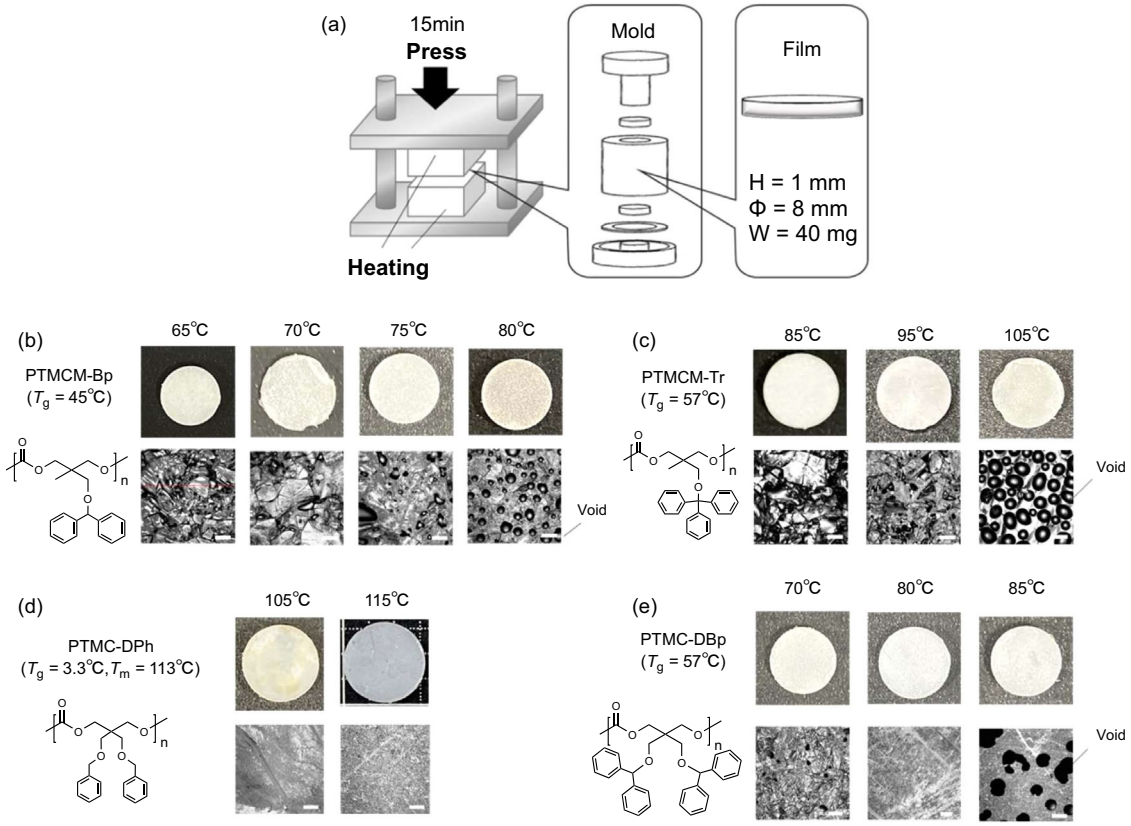

Fig. 3 Schematic illustration showing molding of a film (**a**). Photographs and laser microscopy images of poly(**TMCM-Bp**) films (**b**), poly(**TMCM-Tr**) films (**c**), poly(**TMC-DPh**) films (**d**), and poly(**TMC-DBp**) films (**e**) (scale bar indicates 100 μm)

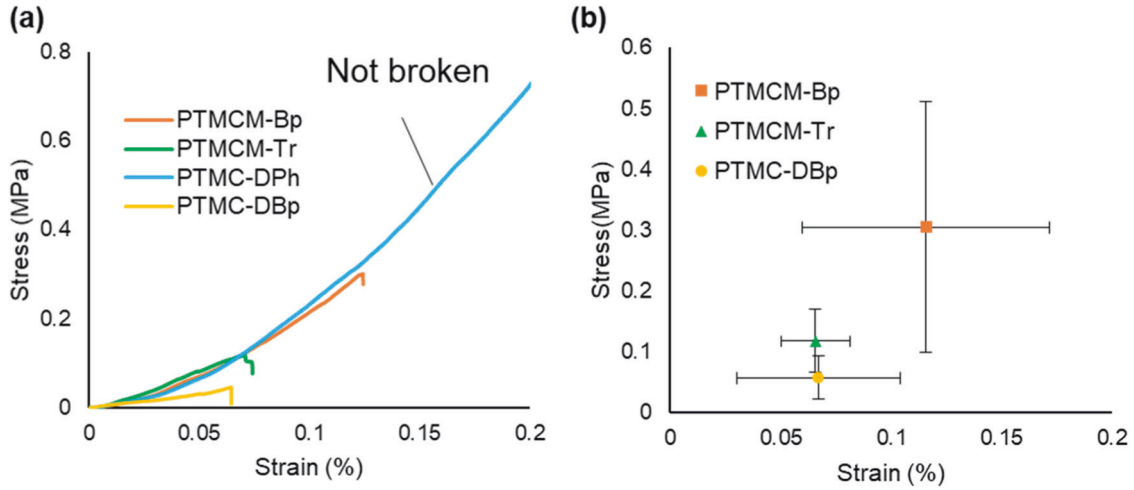

Fig. 4 Stress–strain curves of the PTMC derivatives (**a**). Breaking stress and maximum strain obtained from the stress–strain curves of the PTMC derivatives (**b**)

Table 4 Properties of PTMC derivatives polymerized with *t*-BuOK[a]

Entry	Polymer	M_n[b] ×10^3	DP[b]	M_n[c] ×10^3	DP[c]	T_{10}[d] °C	T_g[e] °C	E[f] MPa	Break strain[g] %	Break Stress[g] MPa
1	Poly(**TMCM-Ph**)	23.5	100	35.4	150	297	–6	N.D.	N.D.	N.D.
2	Poly(**TMCM-Bp**)	21.5	69	40.6	130	281	46	2.30 ± 0.83	0.12 ± 0.06	0.31 ± 0.21
3	Poly(**TMCM-Tr**)	10.2	27	43.5	112	329	57	1.75 ± 0.53	0.07 ± 0.02	0.12 ± 0.06
4	Poly(**TMC-DPh**)	14.3	42	27.4	80	295	3	2.00 ± 0.94	N.D.	N.D.
5	Poly(**TMC-DBp**)	11.0	22	24.7	50	341	57	0.87 ± 0.28	0.07 ± 0.04	0.06 ± 0.04
6	Poly(**TMC-DTr**)	2.5	4	1.9	3	363	73	N.D.	N.D.	N.D.

[a][M]:[I] = 100:1. Initiator = *t*-BuOK. Solvent = THF. Temp. = 0 °C

[b]Determined by SEC in THF and calibrated with PS standards at 40 °C (Table 3)

[c]Determined by ^{1}H NMR

[d]Determined by TGA under nitrogen (10 °C/min.)

[e]Determined by DSC in the second heating cycle (10 °C/min.)

[f]E = Max Stress/Max Strain. Values are means ± standard deviations ($n = 7$). Compression rate = 0.1 mm/min

[g]Values are means ± standard deviations ($n = 7$)

to 0.31 ± 0.21 MPa. In any case, the elastic moduli (E) were almost the same values at 2.0 MPa. These results suggested the polymers were more fragile when they contained large numbers of aromatic groups. The bulky groups present with these molecular weights might have prevented entanglement from contributing to the mechanical strength. The thermal properties and mechanical properties are summarized in Table 4.

Finally, we investigated the degradation of each polymer sample, such as a degradation control by the substituents of other PTMC derivatives [58]. Since it is known that lipase accelerates PTMC hydrolysis and alkaline conditions do not [28] and the OEG substituents in the side chains inhibited hydrolysis [44], we used PBS solutions and aqueous NaOH solutions to study degradation. The 40 mg polymer samples with cylindrical shapes, which are shown in Fig. 3, were placed in 50 mL vials and 40 mL of Lipase PBS solution or 0.01 M aqueous NaOH solutions were added and incubated at 37 °C ($n = 3$). The samples were analyzed with pH measurements after 1, 2, 4, 8, and 12 weeks. The samples were removed from the vials, washed with ion-exchanged water, and then dried at 40 °C overnight. The samples were weighed and photographs and SEM images were obtained, as well as ^{1}H NMR, FT-IR, SEC, TGA, and DSC data. During these experiments, PTMC ($M_n = 13{,}000$) was employed for comparison.

Figure 5 shows weight loss versus time plots for the lipase and alkali treatments. After 12 weeks, the weight losses of poly(**TMCM-Bp**), poly(**TMCM-Tr**), poly(**TMC-DPh**), and poly(**TMC-DBp**) were 0.4%, 1.1%, 1.1%, and 1.4% in the case of the lipase PBS solutions, respectively, although PTMC exhibited a 5.8% loss after 8 weeks

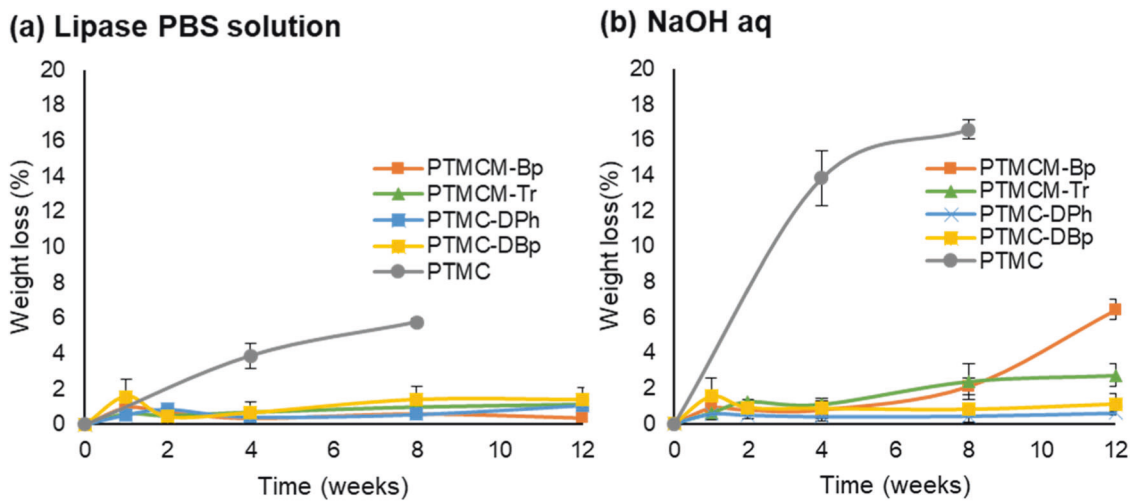

Fig. 5 Weight changes of the PTMC derivatives soaked in the lipase PBS solution (**a**) and in NaOH aq (**b**)

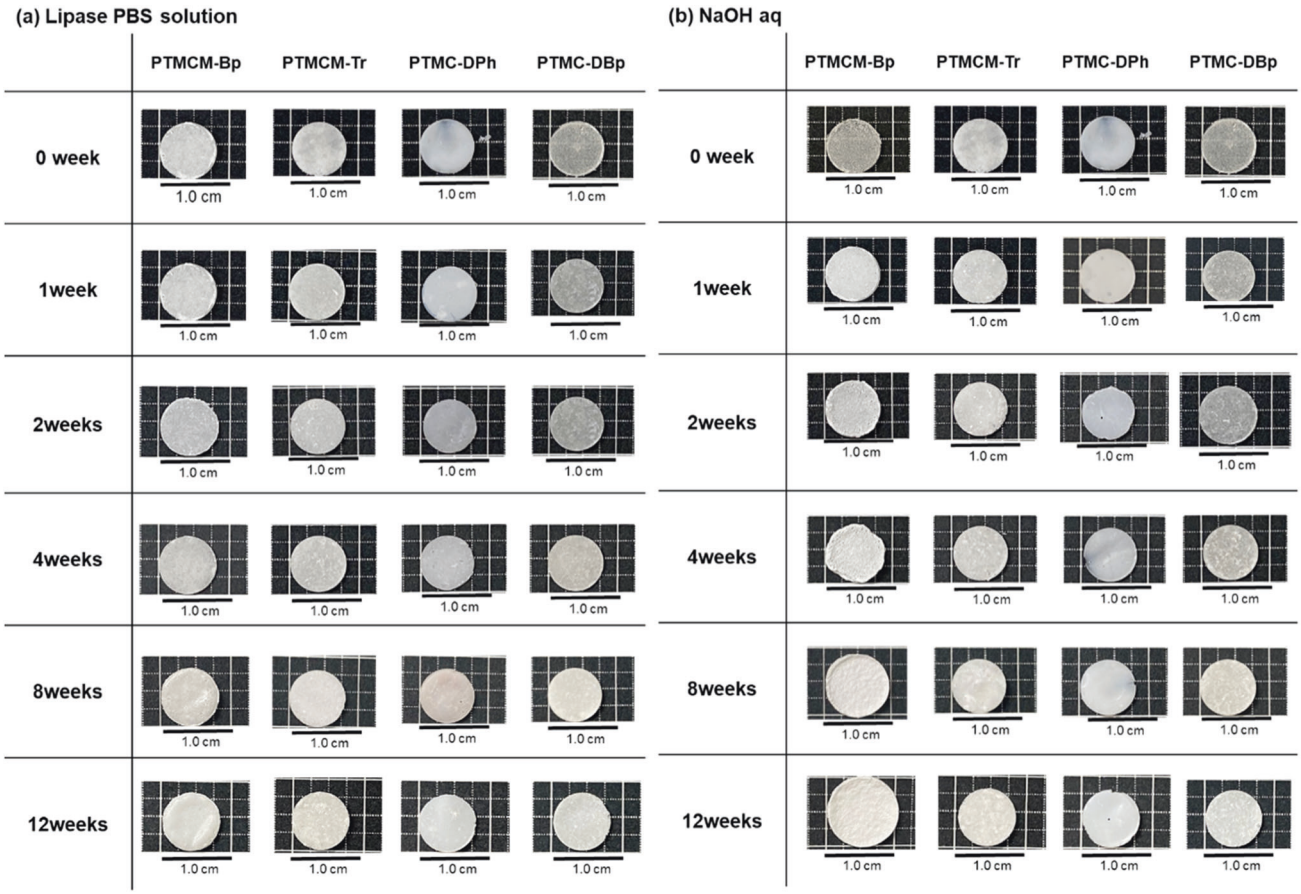

Fig. 6 Appearance of the PTMC derivatives soaked in the lipase PBS solution (**a**) and in the NaOH solution (**b**)

(Fig. 5a). This suggested that the aromatic substituents suppressed hydrolysis; although they are hydrophobic, their bulkiness might have inhibited lipase approach to the carbonyl groups. On the other hand, the weight losses of the polymers were 6.4%, 2.7%, 0.6%, and 1.1% in the case of 0.01 M NaOH, although PTMC exhibited a 16.6% weight loss after 8 weeks (Fig. 5b). Similarly, the aromatic groups inhibited hydrolysis, and two substituents impeded degradation even more. The photographs of the samples are shown in Fig. 6. Most of the shapes looked the same as

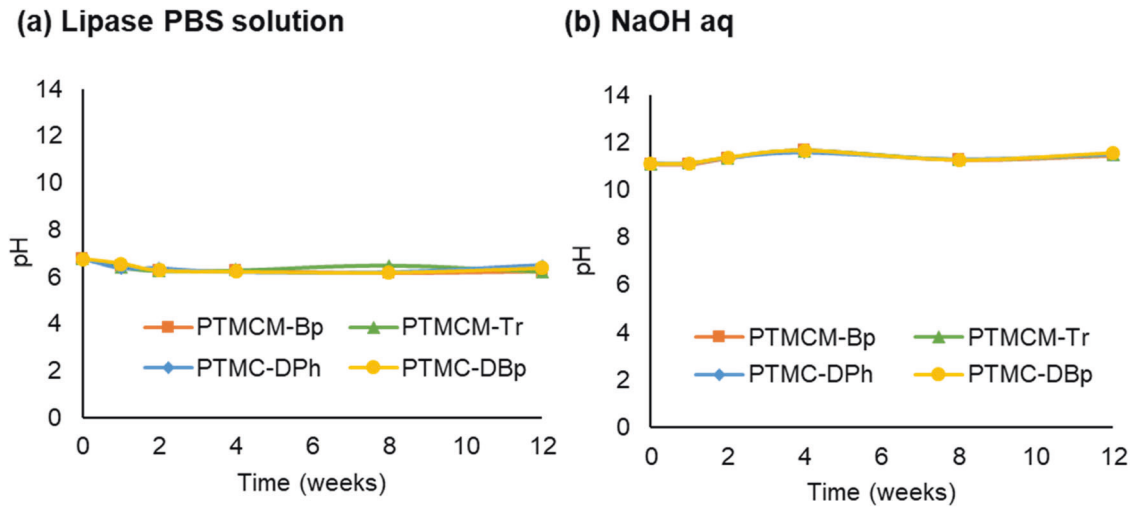

Fig. 7 pH profiles of the lipase PBS solution (**a**) and NaOH solution (**b**) after degradation of the PTMC derivatives

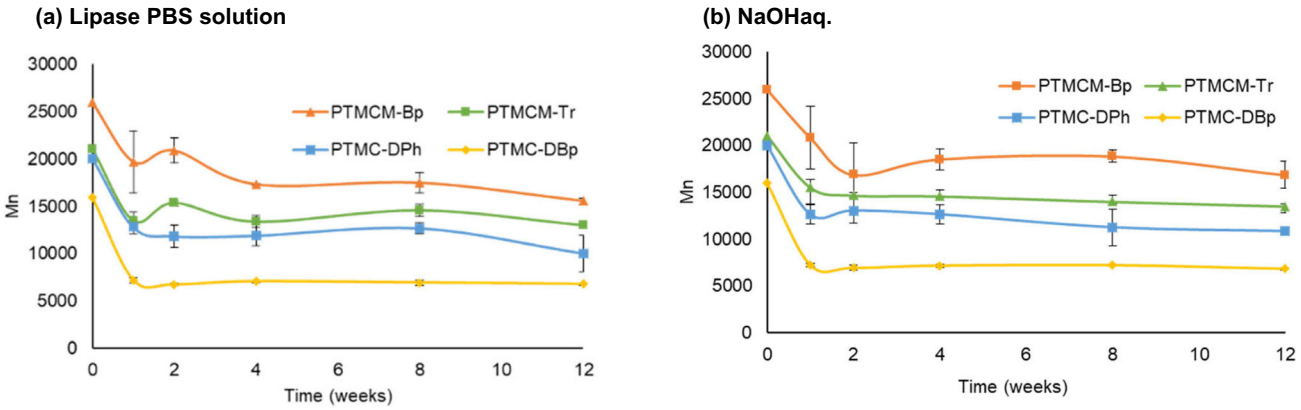

Fig. 8 M_n values determined after soaking in the lipase PBS solution (**a**) and NaOH solution (**b**)

those of the samples before they were dipped in the lipase PBS solution, which should be related to the consistent weights, while the surfaces became slightly white, probably due to a slight amount of degradation (Fig. 6a). Some of the samples became larger after dipping in aqueous NaOH, probably due to flexibilities and resistance to degradation. The surfaces were also white, and the surfaces of poly (**PTMCM-Bp**) became rougher (Fig. 6b). These surface morphologies were observed by SEM, although no specific changes were recognized in any cases (Supplementary Fig. S15).

Figure 7 shows the results of pH measurements with the soluble species produced during the degradation experiments. In both the lipase PBS solutions and NaOH solutions, there were no pH changes, which indicated that the ester-free PTMC derivatives remained neutral during degradation.

The residual samples were dipped into lipase PBS solutions and 0.01 M NaOH and analyzed with ^{1}H NMR (Supplementary Figs. S16–S19) and FT-IR (Supplementary Figs. S20–S23). All of the analyses showed stable polymers, and no specific chemical reactions occurred during the degradation experiments. The M_n values of the residual samples were monitored during the degradation process (Fig. 8), and their SEC traces were also compared (Supplementary Figs. S24 and S25). In both cases, the M_n values for the lipase PBS solutions and NaOH solutions decreased slightly and settled at specific values (Fig. 8a, b), although shoulders generated in the SEC traces after one week (Supplementary Figs. S24 and S25) were consistent with our previous study [44]. Therefore, some degradation occurred in both cases, which indicated that there might be water-insoluble oligomers formed during degradation that were attached to the sample surfaces.

The polymer samples that were dipped into the lipase PBS and NaOH solutions were also analyzed by TGA. It is known that the thermal degradation temperatures of macrocyclic polymers are higher than those of the corresponding linear polymers [59]. Although M_n decreased, the T_{10} value of poly(**TMCM-Bp**) increased after degradation, and

those of poly(**TMC-DPh**) and poly(**TMC-DBp**) increased slightly after immersion in the lipase PBS solutions, whereas the T_{10} for poly(**TMCM-Tr**) decreased (Supplementary Fig. S26). This suggested that the proportion of macrocyclic components in poly(**TMCM-Bp**) was high, as were those for poly(**TMC-DPh**) and poly(**TMC-DBp**). The same tendency for the T_{10} values was observed after immersion in the NaOH solutions (Supplementary Fig. S27). In comparing the conditions of the lipase PBS and NaOH solutions, the T_{10} values increased more after immersion in the lipase PBS solution more than after immersion in the NaOH solution, indicating the possibility of a back biting reaction occurring in the lipase PBS solution [60]. These samples were also analyzed by DSC. It is also known that the T_g values of macrocyclic polymers are higher than those of the corresponding linear polymers [61]. Although the M_n values decreased for all cases during degradation in both the lipase PBS and NaOH solutions, the T_g values for poly(**TMCM-Tr**) and poly(**TMC-DPh**) were the same values as those seen before degradation, while the T_g values for poly(**TMCM-Bp**) and poly(**TMC-DBp**) were lower than those seen before degradation, which was not consistent with the effects assumed for the ratios of the macrocyclic components. Therefore, the thermal properties were not simply related to fundamental factors, such as the chemical structure, polymer structure, and molecular weight.

The soluble products of the degradation experiments were also analyzed to identify the corresponding diol compounds. For example, the ^{1}H NMR spectrum (Supplementary Fig. S30) and FT-IR spectrum (Supplementary Fig. S31) were determined for the soluble product from poly(**TMCM-Bp**) that was produced in the NaOH solution after 12 weeks, which was extracted after neutralization with aqueous HCl. This showed that the degradation process involved hydrolyses of the carbonate groups, as expected.

Conclusion

A series of ester-free TMC derivatives bearing bulky aromatic groups were designed and synthesized. The polymerizations of these monomers with tin initiators and *t*-BuOK were examined, and the processes were optimized to give M_n values over 10,000 in most cases. Compressive tests of poly(**TMCM-Bp**), poly(**TMCM-Tr**), and poly(**TMC-DBp**) resulted in pressures of approximately 0.31 MPa, 0.12 MPa, and 0.06 MPa, respectively, indicating rather soft materials. The degradation behaviors in lipase PBS solutions and 0.01 M NaOH revealed relatively higher stabilities toward hydrolysis than PTMC due to the hydrophobic substituents on the main chains, which remained neutral during hydrolysis.

Data availability

The Supporting Information is available free of charge on the website at DOI: all of the experimental conditions.

Acknowledgements This work was supported by JSPS KAKENHI: Grant-in-Aid for Scientific Research on Innovative Areas (JP22H04547), Grant-in-Aid for Scientific Research (B) (JP20H02799) and Fostering Joint International Research (B) (JP19KK0277). The research was partly supported by The Mazda Foundation (21KK-134). The authors thank Ms. Nishikawa for performing the MALDI-TOF/MS experiments. The authors also appreciate fruitful discussions with Dr. T. Ando, Dr. N. Chanthaset, and H. Yoshida.

Compliance with ethical standards

Conflict of interests The authors declare no competing interests.

References

1. Schneiderman DK, Hillmyer MA. 50th Anniversary perspective: there is a great future in sustainable polymers. Macromolecules. 2017;50:3733–49.
2. Rhodes CJ. Plastic pollution and potential solutions. Sci Prog. 2018;101:207–60.
3. Collignon A, Hecq J-H, Galgani F, Collard F, Goffart A. Annual variation in neustonic micro- and meso-plastic particles and zooplankton in the Bay of Calvi (Mediterranean–Corsica). Mar Pollut Bull. 2014;79:293–8.
4. Maoa R, Langa M, Yua X, Wub R, Yanga X, Guoa X. Aging mechanism of microplastics with UV irradiation and its effects on the adsorption of heavy metals. J Hazard Mater. 2020;393:122515.
5. Gijsman P, Meijers G, Vitarelli G. Comparison of the UV-degradation chemistry of polypropylene, polyethylene, polyamide 6 and polybutylene terephthalate. Polym Degrad Stab. 1999;65:433–41.
6. Driedger AGJ, Dürr HH, Mitchell K, Cappellen PV. Plastic debris in the Laurentian Great Lakes: a review. J Great Lakes Res. 2015;41:9–19.
7. Schmidt C, Krauth T, Wagner S. Export of plastic debris by rivers into the sea. Environ Sci Technol. 2017;51:12246–53.
8. Thompson RC, Olsen Y, Mitchell RP, Davis A, Rowland SJ, John AWG, et al. Lost at sea: where is all the plastic. Science. 2004;304:5672–838.
9. He L, Wu D, Rong H, Li M, Tong M, Kim H. Influence of nano- and microplastic particles on the transport and deposition behaviors of bacteria in quartz sand. Environ Sci Technol. 2018;52:11555–63.
10. Lin VS. Research highlights: impacts of microplastics on plankton. Environ Sci Processes Impacts. 2016;18:160–3.
11. Ivleva NP, Wiesheu AC, Niessner R. Microplastic in aquatic ecosystems. Angew Chem Int Ed. 2017;56:1720–39.
12. Barboza LGA, Vieira LR, Branco V, Carvalho C, Guilhermino L. Microplastics increase mercury bioconcentration in gills and bioaccumulation in the liver, and cause oxidative stress and damage in Dicentrarchus labrax juveniles. Sci Rep. 2018;8:15655.

13. Raamsdonk LWDV, Zande MVD, Koelmans AA, Hoogenboom RLAP, Peters RJB, Groot MJ, et al. Current insights into monitoring, bioaccumulation, and potential health effects of microplastics present in the food chain. Foods. 2020;9(9):72.
14. Iwata T. Biodegradable and bio-based polymers: future prospects of eco-friendly plastics. Angew Chem Int Ed. 2015;54:3210–5.
15. Haider TP, Vçlker C, Kramm J, Landfester K, Wurm FR. Plastics of the future? The impact of biodegradable polymers on the environment and on society. Angew Chem Int Ed. 2019;58:50–62.
16. Jamshidian M, Tehrany EA, Imran M, Jacquot M, Desobry S. Poly-lactic acid: production, applications, nanocomposites, and release studies. Compr Rev Food Sci Food Saf. 2010;9:552–71.
17. Tan GYA, Chen CL, Li L, Ge L, Wang L, Razaad IMN, et al. Start a research on biopolymer polyhydroxyalkanoate (PHA): a review. Polymers. 2014;6:706–54.
18. Li H, Chang J, Cao A, Wang J. in vitro evaluation of biodegradable poly(butylene succinate) as a novel biomaterial. Macromol Biosci. 2005;5:433–40.
19. Jem KJ, Tan B. The development and challenges of poly (lactic acid) and poly (glycolic acid). Adv Ind Eng Polym. Res. 2020;3:60–70.
20. Yamane K, Sato H, Ichikawa Y, Sunagawa K, Shigaki Y. Development of an industrial production technology for high-molecular-weight polyglycolic acid. Polym J. 2014;46:769–75.
21. Bhattacharjee P, Naskar D, Kim HW, Maiti TK, Bhattacharya D, Kundu SC. Non-mulberry silk fibroin grafted PCL nanofibrous scaffold: Promising ECM for bone tissue engineering. Eur Polym J. 2015;71:490–509.
22. Someya Y, Sugahara Y, Shibata M. Nanocomposites based on poly(butylene adipate-co-terephthalate) and montmorillonite. J Appl Polym Sci. 2005;95:386–92.
23. Mitsuki T, Tanaka C., Nemoto T. Japan Patent, JP2023-110831A.
24. Song J, Dou Y, Niu Y, He N. Properties of HA/PBS biodegradable film and evaluation of its influence on the growth of vegetables. Polym Test. 2021;95:107137.
25. Towata R. Japan Patent, JP2020-127410A.
26. Xu X, Zhang J, Filion TM, Akalin A, Song J. Modulating mechanical and shape-memory properties while mitigating degradation-induced inflammation of polylactides by pendant aspirin incorporation. ACS Appl Mater Interfaces. 2021;13: 22271–81.
27. Shen Y, Tu T, Yi B, Wang X, Tang H, Liu W, et al. Electrospun acid-neutralizing fibers for the amelioration of inflammatory response. Acta Biomater. 2019;97:200–15.
28. Zhanga Z, Kuijer R, Bulstrab SK, Grijpma DW, Feijen J. The in vivo and in vitro degradation behavior of poly(trimethylene carbonate. Biomaterials. 2006;27:1741–8.
29. Pêgo AP, Grijpma DW, Feijen J. Enhanced mechanical properties of 1,3-trimethylene carbonate polymers and networks. Polymer. 2003;44:6495–504.
30. Yang L, Li J, Zhang W, Jin Y, Zhang J, Liu Y, et al. The degradation of poly(trimethylene carbonate) implants: the role of molecular weight and enzymes. Polym Degrad Stab. 2015;122:77–87.
31. Tempelaar S, Mespouille L, Coulembier O, Duboisb P, Dove AP. Synthesis and post-polymerization modifications of aliphatic poly(carbonate)s prepared by ring-opening polymerisation. Chem Soc Rev. 2013;42:1312–36.
32. Yang J, Tian W, Li Q, Li Y, Cao A. Novel biodegradable aliphatic poly(butylene succinate-co-cyclic carbonate)s bearing functionalizable carbonate building blocks: II. Enzymatic biodegradation and in vitro biocompatibility assay. Biomacromolecules. 2004;5:2258–68.
33. Albertsson AC, Eklund M. Influence of molecular structure on the degradation mechanism of degradable polymers: In vitro degradation of poly(trimethylene carbonate), poly(trimethylene carbonate-co-caprolactone), and poly(adipic anhydride). J Appl Polym Sci. 1995;57:87–103.
34. Song Y, Kamphuis MMJ, Zhang Z, et al. Flexible and elastic porous poly(trimethylene carbonate) structures for use in vascular tissue engineering. Acta Biomater. 2010;6:1269–77.
35. Papenburg BJ, Schüller-Ravoo S, Bolhuis-Versteeg LA, Hartsuiker L, Grijpma DW, Feijen J, et al. Designing porosity and topography of poly(1,3-trimethylene carbonate) scaffolds. Acta Biomater. 2009;5:3281–94.
36. Riahinezhad H, Kerr-Dini N, Amsden BG. Degradation of poly(vinyl sulfone carbonate) in aqueous media. Polym Degrad Stab. 2023;216:110472.
37. Zhang W, Hou Z, Chen S, Guo J, Hu J, Yang L. et al. Aspergillus oryzae lipase-mediated in vitro enzymatic degradation of poly (2,2′-dimethyltrimethylene carbonate-co-ε-caprolactone). Polym Degrad Stab. 2023;211:110340.
38. Fukushima K, Watanabe Y, Ueda T, Nakai S, Kato T. Organocatalytic depolymerization of poly(trimethylene carbonate). J Polym Sci. 2022;60:3489–3500.
39. Yu W, Maynard E, Chiaradia V, Arno MC, Dove AP. Aliphatic polycarbonates from cyclic carbonate monomers and their application as biomaterials. Chem Rev. 2021;121:10865–907.
40. Ansari I, Singh P, Mittal A, Mahato RI, Chitkara D. 2,2-Bis(hydroxymethyl) propionic acid based cyclic carbonate monomers and their (co)polymers as advanced materials for biomedical applications. Biomaterials. 2021;275:120953.
41. Fukushima K. Poly(trimethylene carbonate)-based polymers engineered for biodegradable functional biomaterials. Biomater Sci. 2016;4:9–24.
42. Chanthaset N, Ajiro H. Preparation of thermosensitive biodegradable hydrogel using poly(5-[2-{2-(2-methoxyethoxy) ethyoxy}-ethoxymethyl]-5-methyl-1,3-dioxa-2-one) derivatives. Materialia. 2019;5:100178.
43. Ajiro H, Takahashi Y, Akashi M. Thermosensitive biodegradable homopolymer of trimethylene carbonate derivative at body temperature. Macromolecules. 2012;45:2668–74.
44. Haramiishi Y, Chanthaset N, Kan K, Akashi M, Ajiro H. Contrast effect on hydrolysis of poly(trimethylene carbonate) depending on accelerated species due to the hydrophilic oligo(ethylene glycol) units at side groups. Polym Degrad Stab. 2016;130:78–82.
45. Nobuoka H, Ajiro H. Nobuoka H, Ajiro H. Biodegradable and biocompatible crosslinked film with trimethylene carbonate bearing oligo(ethylene glycol). Chem Lett. 2019;48:245–8.
46. Nobuoka H, Ajiro H. Novel synthesis method of ester free trimethylene carbonate derivatives. Tetrahedron Lett. 2019;60: 164–70.
47. Miyake R, Maehara A, Chanthaset N, Ajiro H. Thermal property control by copolymerization of trimethylene carbonate and its derivative bearing triphenylmethyl group. ChemistrySelect. 2022;7:e202104326.
48. Nobuoka H, Ajiro H. Development of ester free type poly(-trimethylene carbonate) derivatives with pendant fluoroaromatic groups. Macromol Chem Phys. 2019;220:1900051.
49. Ouchi M, Inoue Y, Wada K, Iketani S, Kakushi T, Weber E. Molecular design of crown ethers. 4. Syntheses and selective cation binding of 16-crown-5 and 19-crown-6 lariats. J Org Chem. 1987;52:2420–7.
50. Weber E. Polytopic cation receptors. 2. Synthesis and selective complex formation of spiro-linked "multiloop crown compounds. J Org Chem. 1982;47:3478–86.
51. Nederberg F, Lohmeijer BGG, Leibfarth F, Pratt RC, Choi J, Dove AP, et al. Organocatalytic ring opening polymerization of trimethylene carbonate. Biomacromolecules. 2007;8:153–60.
52. Kricheldorf HR, Stricker A. Polymers of carbonic acid, 28. SnOct2-initiated polymerizations of trimethylene carbonate (TMC, 1,3-dioxanone-2. Macromol Chem Phys. 2000;201:2557–65.

53. Kricheldorf HR, Stricker A. Polymers of carbonic acid 29. Bu 2 SnOct 2 —initiated polymerizations of trimethylene carbonate (TMC, 1,3-dioxanone-2. Polymer. 2000;41:7311–20.
54. Albertsson AC, Sjöling M. Homopolymerization of 1,3-dioxan-2-one to high-molecular-weight poly(trimethylene carbonate). J Macromol Sci Pure Appl Chem. 1992;A29:43–54.
55. Nakazono K, Yamashita C, Ogawa T, Iguchi H, Takata T. Synthesis and properties of pendant fluorene moiety-tethered aliphatic polycarbonates. Polym J. 2015;47:355–61.
56. Matsuo J, Aoki K, Sanda F, Endo T. Substituent effect on the anionic equilibrium polymerization of six-membered cyclic carbonates. Macromolecules. 1998;31:4432–8.
57. Brissenden AJ, Amsden BG. Insights into the polymerization kinetics of thermoresponsive polytrimethylene carbonate bearing a methoxyethoxy side group. J Polym Sci. 2020;58:2697–707.
58. Prinse M, Qi R, Amsden BG. Polymer micelles for the protection and delivery of specialized pro-resolving mediators. Eur J Pharm Biopharm. 2023;184:159–69.
59. Hong M, Chen EYX. Completely recyclable biopolymers with linear and cyclic topologies via ring-opening polymerization of γ-butyrolactone. Nat Chem. 2016;8:42–9.
60. Aris MH, Annuar MSM, Ling TC. Lipase-mediated degradation of poly-ε-caprolactone in toluene: behavior and its action mechanism. Polym Degrad Stab. 2016;133:182–91.
61. Yamamoto T, Tezuka I. Topological polymer chemistry: new synthesis of cyclic and multicyclic polymers and topology effects thereby. Kobunshi Ronbunshu. 2011;68:782–94.